Supporting Information

**Enhanced Conduction and Charge-Selectivity by N-Doped Graphene Flakes in the Active Layer of Bulk Heterojunction Organic Solar Cell**

Gwang Hoon Jun,[a] Sung Hwan Jin,[a] Bo Hyun Kim,[a] Weon-Sik Chae,[b] Soon Hyung Hong*[a] and Seokwoo Jeon*[a]

a Department of Material Science & Engineering, Graphene Research Center (GRC),

KAIST Insti-tute for the Nano-century, Korea Advanced Institute of Science and Technology

(KAIST), 291 Daehak-ro, Yuseong-gu, Daejeon 305-701, Korea

b Gangneung Center, Korea Basic Science Institute, Gangneung 210-702, Korea

KEYWORDS graphene, nitrogen doping, organic photovoltaic, bulkheterojunction
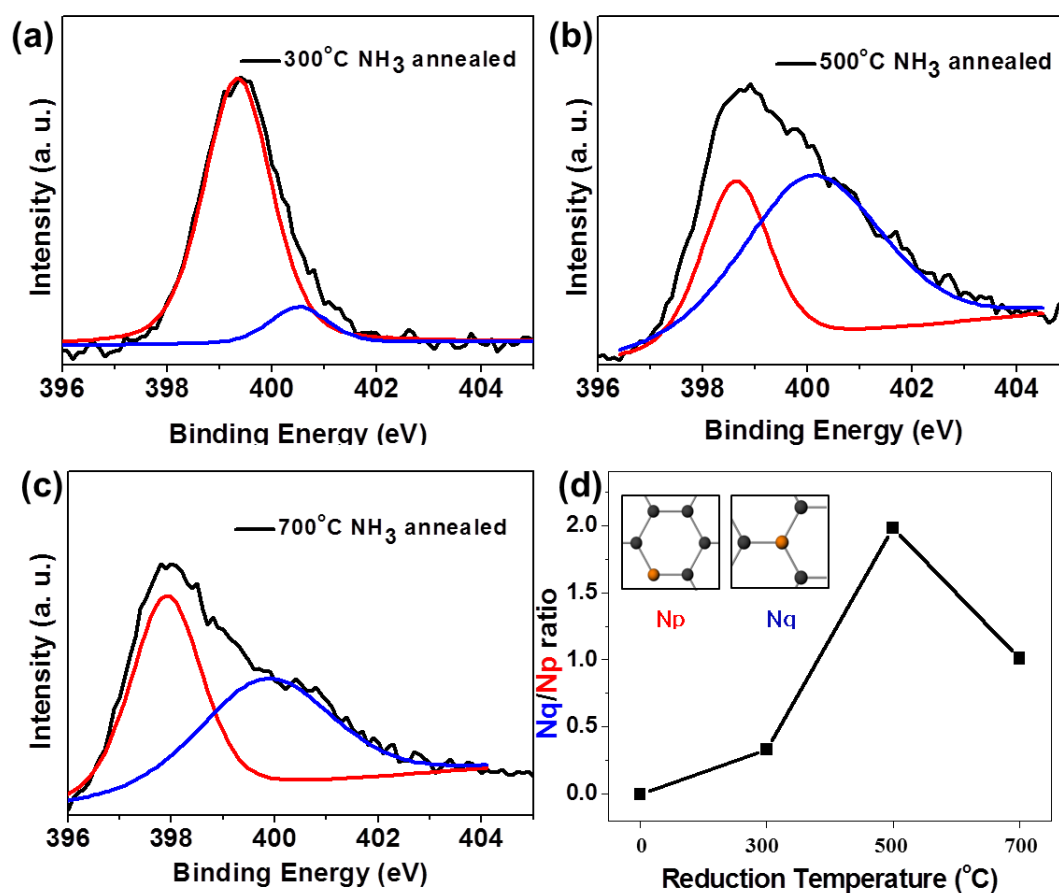
Fig. 1 XPS spectra of N (1s) peaks. High resolution N (1s) spectra of RGO by reduced in NH3 at different temperatures. 300 ℃ (a), 500 ℃ (b) and 700 ℃ (c). Pyridinic N (Np)/ quaternary N (Nq) ratio in reduced graphene as a function of the thermal reduction temperature. (d)

Fig. S1 shows high-resolution N1s XPS analysis of the bonding configurations of N atoms in reduced graphene oxide with various heat-treatment temperatures. Each N1s peak was resolved into three peaks: the lowest energy peak near 398.8~399.1 eV corresponded to pyridinic N (N_{pyri}), and the energy peak at 400.5~400.7 eV represented quaternary N (N_{qua}).[R1,R2] It is well known that only N_{qua} improves the electroconductivity of graphene films. N_{pyri}, with its localized lone pair of electrons (Fig. S1d, inset atomic structures), inevitably is accompanied by vacancy defects and cannot contribute to the recovery of the graphitic structure. In contrast, N_{qua}, a secure substitution of C with N (Fig. 3(a), upper left), is known to maintain a sp2-hybridized graphitic structure; it also provides delocalized electrons to enhance electroconductivity.

.
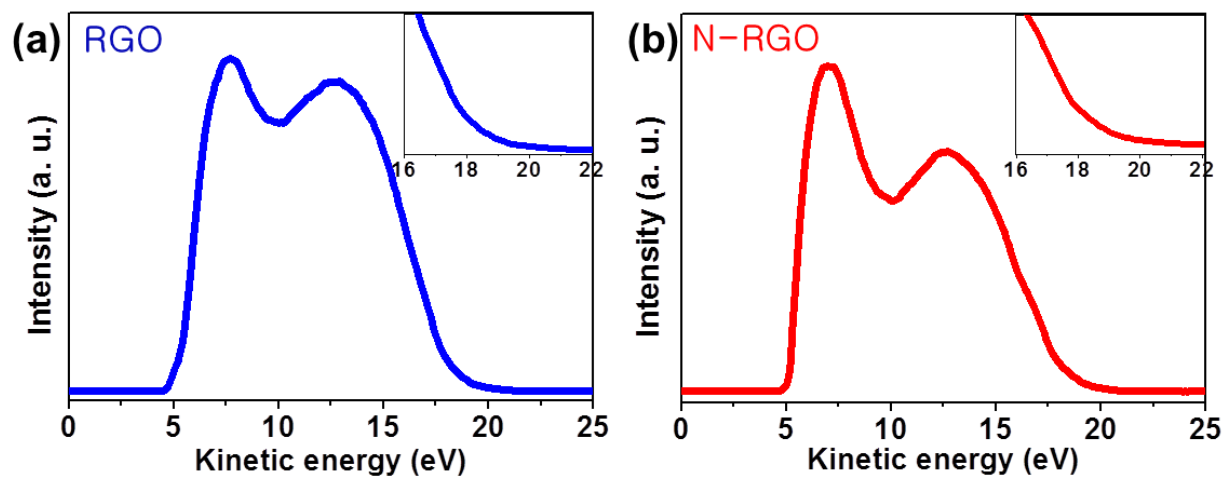
Fig. S2 Work functions of (a) undoped RGO and (b) nitrogen doped N-RGO determined by UPS measurements with He I (hv =21.2 eV)

source.

From the UPS spectra, the work function was taken as the difference in energy level between the inelastic cutoff and the Fermi edge. The calculated work function of undoped RGO was Φ = 21.2 eV − (21 eV − 4.6 eV) = 4.8 eV, and that of N-RGO was Φ = 21.2 eV − (21.4 eV − 5 eV) = 4.4 eV.
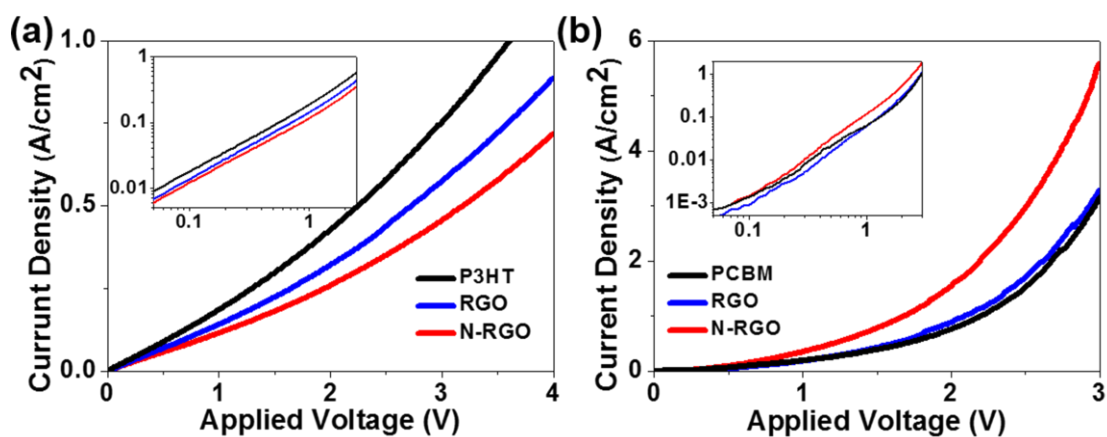
Fig. S3 I – V characteristics of a) P3HT only and b) PCBM only devices (insets : logarithmic scales)

To investigate the effect of the increase in charge-carrier mobility caused by the incorporated N-RGO, we characterized mobility using the Mott–Gurney law[R3, R4] :

$$J = \frac{9}{8} \varepsilon_r \varepsilon_0 \mu \frac{V^2}{L^3}$$ (R1)

where ε_r is the relative dielectric constant, ε_0 is the permittivity of the free space, μ is the charge-carrier mobility, V is the applied voltage, and L is the thickness of the device. The electron mobility increased by ~74% (3.1×10^{-7} to 5.4×10^{-7} m^2 V^{-1}s^{-1}). This improvement in the mobility resulted from the fact that the graphenes acted as effective charge-carrier pathways due to their high electrical conductivity.
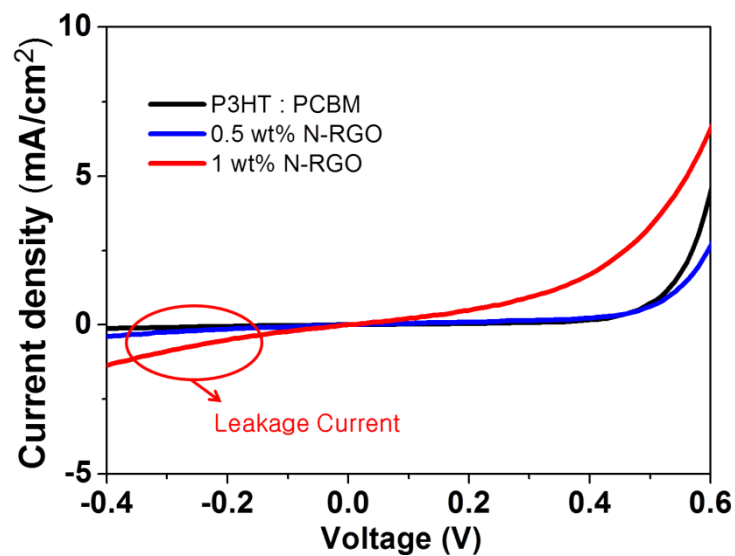
Fig. S4 Current density–voltage (I–V) characteristics of devices without light illumination (dark state).

To confirm the tendency toward increased leakage current from samples with overweight concentrations of N-RGO, we performed I–V characterization without light illumination. Ideally, a solar cell without light illumination has no current density with a negative voltage due to the properties of the donor–acceptor junction. However, a device using N-RGO/P3HT:PCBM exhibited some leakage current. In contrast, a device using P3HT:PCBM showed no current with a negative voltage. This leakage current could affect the diode behavior and decrease the FF and PCE.
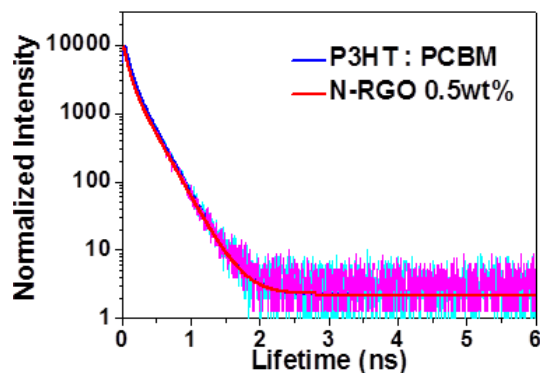
Fig. S5 Normalized fluorescence-lifetime curve of P3HT : PCBM (blue line) and incorporated 0.5 wt% of N-RGO (red line).

Fig. S5 shows the normalized fluorescence decay curves of P3HT:PCBM and 0.5 wt% N-RGO/P3HT:PCBM. No significant change was observed in the lifetime by incorporation of N-RGO (0.235 ± 0.001, n.s., and 0.238 ± 0.002, n.s. for P3HT:PCBM and 0.5 wt% N-RGO/P3HT:PCBM, respectively).

From these time-resolved PL intensity and lifetime studies, our results showed that the graphene flakes played the role of charge-carrier pathways rather than exciton dissociation sites. This was verified by the PL lifetime, with no significant change observed with incorporation of N-RGO, as indicated in Fig. S5. This suggests that the work function difference of donor/acceptor P3HT/PCBM is larger than that of donor/N-RGO; thus, the excitons are mainly dissociated at donor/acceptor interfaces.

Table S1. Atomic concentration of graphite, GO, RGO, and N-RGO

	C (atomic %)	O (atomic %)	N (atomic %)	C/O ratio
Graphite	99.44	0.56		
GO	63.18	32.65	1.55	1.94
RGO	88.78	11.22	-	7.91
N-RGO	86.52	5.19	7.44	16.67

Table S2. Proportion of N-P and N-Q with various thermal reduction temperatures

	N-P (%)	N-Q (%)	Ratio (Nq/Np)
300 $^{\circ}$C	75	25	0.33
500 $^{\circ}$C	33	66	1.98
700 $^{\circ}$C	49	51	1.01

Table S3. Photovoltaic parameters of OPV cells of RGO/P3HT:PCBM and N-RGO/P3HT:PCBM in this work

	J_{SC} [mA/cm^2]	V_{OC} [V]	FF	PCE [%]
Pristine P3HT:PCBM	10.54 ± 0.11	0.58 ± 0.01	0.51 ± 0.01	3.12 ± 0.07
RGO 0.1wt%	12.69 ± 0.31	0.53 ± 0.01	0.40 ± 0.01	2.71 ± 0.17
RGO 0.5wt%	7.37 ± 0.29	0.54 ± 0.01	0.40 ± 0.01	1.61 ± 0.09
RGO 1wt%	6.57 ± 0.10	0.45 ± 0.01	0.38 ± 0.01	1.06 ± 0.03
N-RGO 0.1wt%	12.96 ± 0.41	0.56 ± 0.01	0.50 ± 0.01	3.65 ± 0.19
N-RGO 0.5wt%	14.86 ± 0.09	0.58 ± 0.01	0.50 ± 0.01	4.39 ± 0.09
N-RGO 1wt%	14.86 ± 0.58	0.58 ± 0.02	0.46 ± 0.03	4.06 ± 0.29

Table S4. Charge carrier motilities: PCBM-only devices (electron) and P3HT-only devices (hole). The concentration of graphene is 1 wt%

	Electron mobility (PCBM only devices) (m^{2}V^{-1}s^{-1})	Hole mobility (P3HT only devices) (m^{2}V^{-1}s^{-1})
without graphene	3.1×10^{-7}	7.3×10^{-8}
RGO	3.2×10^{-7}	5.6×10^{-8}
N-RGO (1 wt%)	5.4×10^{-7}	4.4×10^{-8}

References

R1 X. L. Li, H. L. Wang, J. T. Robinson, H. Sanchez, G. Diankov and H. J. Dai, *J Am Chem Soc*, 2009, **131**, 15939-15944.

R2 H. M. Jeong, J. W. Lee, W. H. Shin, Y. J. Choi, H. J. Shin, J. K. Kang, and J. W. Choi, *Nano Lett*., 2011, **11**, 2472-2477

R3 V. D. Mihailetchi, J. K. J. van Duren, P. W. M. Blom, J. C. Hummelen, R. A. J. Janssen, J. M. Kroon, M. T. Rispens, W. J. H. Verhees, M. M. Wienk, *Adv. Funct. Mater*., 2003, **13**, 43-46.

R4 S. Scheinert, W. Schliefke, *Synt. Met*., 2003, **139**, 501-509.